Journal of Membrane Science 451 (2014) 205–215

Contents lists available at ScienceDirect

Journal of Membrane Science

journal homepage: www.elsevier.com/locate/memsci

Surface coating on the polyamide TFC RO membrane for chlorine resistance and antifouling performance improvement

Lei Ni, Jianqiang Meng*, Xiaogang Li, Yufeng Zhang

State Key Laboratory of Hollow Fiber Membrane Materials and Processes, Tianjin Polytechnic University, Tianjin 300387, P.R. China

ARTICLE INFO

Article history:
Received 26 May 2013
Received in revised form
18 September 2013
Accepted 21 September 2013
Available online 2 October 2013

Keywords:
Surface coating
Reverse osmosis (RO)
Thin-film composite membrane (TFC)
Chlorine resistance
Antifouling

ABSTRACT

A novel random terpolymer poly(methylacryloxyethyldimethyl benzyl ammonium chloride-*r*-acrylamide-*r*-2-hydroxyethyl methacrylate) (P(MDBAC-*r*-Am-*r*-HEMA)) was synthesized via free radical polymerization and used as the coating material on the polyamide thin film composite (TFC) reverse osmosis (RO) membrane to improve its chlorine resistance and antifouling performance. The chlorine resistance of the membranes was evaluated by cross-flow filtration of the NaClO solution. Antifouling performance was evaluated by cross-flow filtration of the protein solution and cell-culture experiments. The membrane surface was analyzed via ATR-FTIR, XPS, SEM and streaming potential measurements. The coated membrane can tolerate chlorine exposure over 16,000 ppm h, which is 7–10 times the pristine membrane. The bacteria growth can be significantly depressed on the coated membrane surface. The coated membrane can retain its flux very well under protein filtration. It is believed that the surface coating layer works as a protective and sacrificial layer, preventing the attack of chlorine on the underlying polyamide film. The PMDBAC and PAm components are essential to the antimicrobial property and the improved surface hydrophilicity is beneficial to the antifouling performance of the membrane. The coated membrane offers potential use as a novel RO membrane with improved antifouling performance and chlorine resistance.

1. Introduction

With the worldwide population growth, industrialization and urbanization, there is an increasing demand for freshwater. In contrast, many freshwater resources are becoming unavailable due to pollution and industrial activities. The water scarcity problem is expected to become more and more severe in the coming decades. Desalination has been considered as one of the most important methods to relieve this issue. As the mainstream desalination technology, reverse osmosis (RO) accounts for 59.85% of the total worldwide installed capacity for desalination until 2011[1].

Polyamide (PA) thin film composite (TFC) membrane has been predominating the commercial RO membrane market since nearly 30 years [2]. It has a multilayer structure of interfacially polymerized polyamide (PA) thin film supported by a microporous polymeric membrane. The ultrathin barrier layer and the support can be independently optimized to combine high water permeability and high salt rejection [3–5]. However, this kind of RO membrane has two drawbacks, limiting its wide application and long-term performance. The first drawback is its proneness to fouling from all kinds of matters in the influent. Therefore critical pretreatment conditions and frequent membrane rinse are required, which lead to significant capital and energy cost. The second drawback is its vulnerability to chlorine, which is the most widely used disinfectant in water treatment for biofouling control. The membrane dramatically loses its salt rejection characteristics when exposed to even a few parts per million of chlorine.

The proneness to fouling for the TFC RO membrane is believed to be related to its insufficient hydrophilicity and high roughness [6,7]. The RO membrane fouling can be categorized into four mechanisms: mineral deposition, organic fouling, colloidal fouling and biofouling. Among them, biofouling is mostly troublesome and is the major cause of RO fouling [8]. In this context, anti-biofouling membranes have been developed by introducing polycations onto membrane surfaces. It has been demonstrated that polycation hybrid membranes have good antimicrobial properties, which can destroy microorganisms [9,10]. On the other hand, non-specific adhesion is the start of almost all of the fouling mechanisms and processes. Therefore, various hydrophilic polymers containing hydroxy, carbonyl or ethylene oxide groups have been coated or grafted on the membrane surface towards antifouling RO membranes [4]. Although more permanent surface modification can be achieved by surface grafting, surface coating is more convenient and easier to be implemented on a large scale.

Membrane vulnerability to chlorine is due to the presence of chlorine-sensitive sites in the PA film such as amide nitrogen and aromatic rings [11–13]. Numerous attempts have therefore been made to develop RO membranes having improved antifouling performance and chlorine resistance. Novel methods totally different

* Corresponding author. Tel.: +86 22 83955078; fax: +86 22 83955055.
E-mail address: jianqiang.meng@hotmail.com (J. Meng).

0376-7388/$ - see front matter © 2013 Elsevier B.V. All rights reserved.
http://dx.doi.org/10.1016/j.memsci.2013.09.040

from PA chemistry have been developed to prepare chlorine-resistant RO membranes [5,14]. Tailoring of the PA skeleton to eliminate chlorine-sensitive sites is another approach to synthesize novel chlorine-resistant PA RO membranes [15]. These membranes have shown excellent chlorine resistance. However, they have not shown potential to be competitive with state-of-the-art commercial membranes on salt rejection performance and fabrication convenience. Surface modifications such as surface coating and surface grafting are potential methods to improve membrane chlorine-resistance properties. They are easier to implement, can effectively vary membrane surface properties and hence are more persuasive to the industry. It has been reported that the chlorine resistances of the aromatic polyamide RO membranes can be improved by coating with polymers as protective layers [16–18], which cover the sensitive sites of aromatic polyamides or sacrificial layers [19,20], thereby protecting them from chlorine attack.

Considering this, we designed a novel hydrophilic random copolymer poly(methylacryloxyethyldimethyl benzyl ammonium chloride-*r*-acrylamide-*r*- 2-hydroxyethyl methacrylate) (P(MDBAC -*r*-Am-*r*-HEMA)), which was used as a coating material to improve membrane antifouling performance and chlorine resistance. The terpolymer comprises methylacryloxyethyldimethyl benzyl ammo -nium chloride (MDBAC), acrylamide (Am) and 2-hydroxyethyl methacrylate (HEMA) and was synthesized via simple free-radical copolymerization. The terpolymer was coated on a commercial RO membrane followed by glutaraldehyde (GA) cross-linking. Synthesis of the terpolymer, chemical structure of the PA layer and coating chemistry are elucidated in Scheme 1. Chemical compositions and morphologies of the modified membranes were characterized via ATR-FTIR, XPS, SEM and AFM. The physicochemical properties of the membrane surface were characterized via water contact angle (WCA) and streaming potential measurements. The permeation and salt rejection properties were measured with a cross-flow testing bench. The antifouling and chlorine-resistant properties were evaluated systematically.

2. Experimental

2.1. Materials and reagents

Commercial TFC RO membranes (LCLE and BW30) were purchased from DOW Chemical Co. Ltd. (Minneapolis, MN, USA). LCLE membrane is a low-energy RO membrane product and BW30 is a standard brackish water RO membrane product. Both membranes were declared by the vendor to have PA TFC structures. The monomer MD BAC was synthesized according to the method reported in the literature [6,9]. Azodiisobutyronitrile (AIBN), N, N-dimethylaminoethyl, methacrylate (DMAEMA), benzyl chloride, acrylamide, dimethyl sulfone (DMSO), glutaraldehyde (GA) and 2-hydroxyethyl methacrylate were purchased from Sigma-Aldrich. Sodium hypochlorite solution (NaClO, 6 wt% free chlorine) used in membrane chlorine exposure

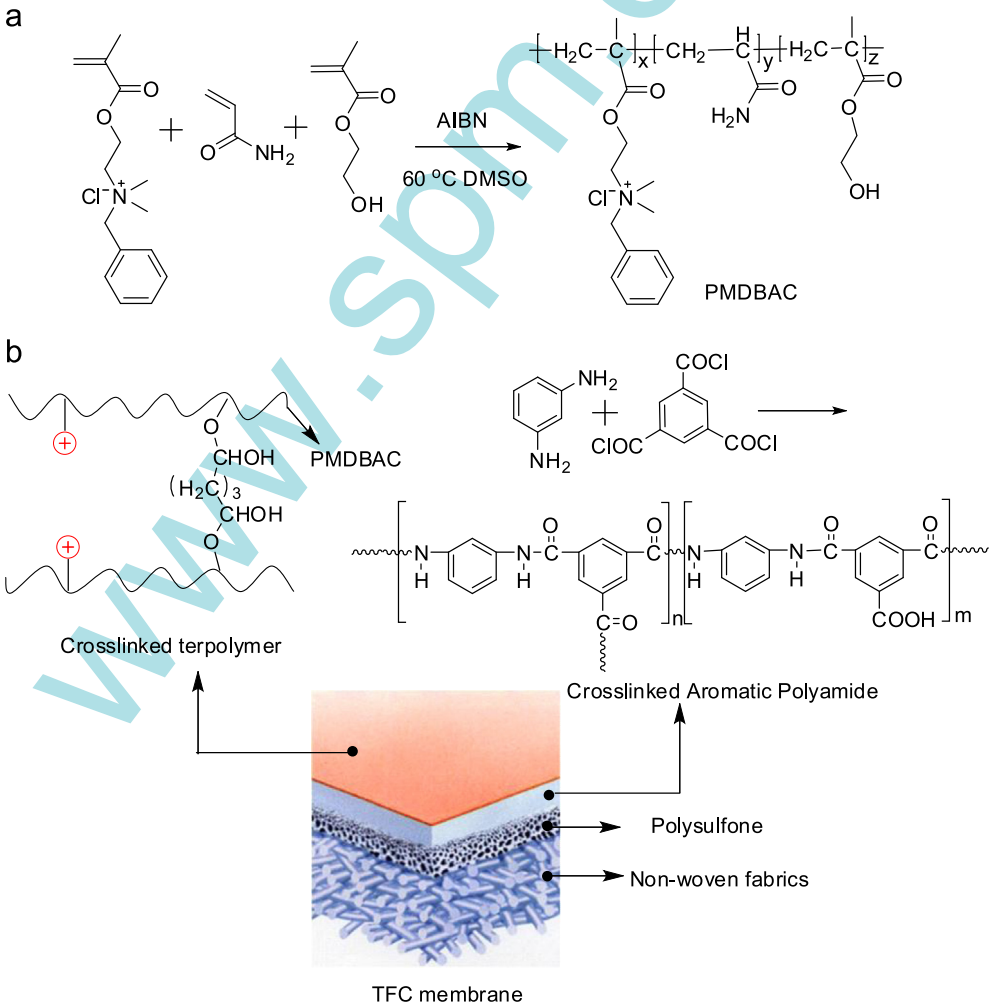

Scheme 1. Schematic diagram for synthesis of the terpolymer P(MDBAC-*r*-Am-*r*-HEMA) (a) and surface modification of RO membranes (b).

experiments was purchased from Kermel Chemical Reagent Co. Ltd. (Tianjin, China). All the other chemicals and reagents were used as received without any purification.

2.2. Synthesis and characterization of P(MDBAC-r-am-r-HEMA)

The hydrophilic copolymer, P(MDBAC-*r*-Am-*r*-HEMA), was synthesized via the free radical copolymerization of MDBAC, Am and HEMA in DMSO solution (Scheme 1). Typically, 5.68 g (20 mmol) of MDBAC, 1.42 g (20 mmol) of Am and 2.60 g of HEMA (20 mmol) were dissolved in 60 mL of DMSO. Then 0.10 g (0.6 mmol) of AIBN was added after purging with nitrogen for 30 min at 25 °C. The polymerization was conducted at 60 °C for 7 h. The crude product was obtained as a white precipitate by precipitating from ethylether. The final product P(MDBAC-*co*-Am-*co*-HEMA) was purified by redissolving in DMSO and re-precipitating in ethylether and lyophilized at −60 °C.

The chemical structure of the copolymer was analyzed by ^{1}H NMR using a Bruker 400-MHz spectrometer with D_2O as the solvent. The molecular weight (M_w) of the copolymer was analyzed by multi-angle laser light scattering (MALLS). The copolymer was dissolved in DI H_2O to the final concentrations of 1.00, 0.80, 0.60, 0.40, 0.20 and 0.10 mg/mL. After filtration (0.45 μm), the molecular weight was determined at 532 nm with test angle from 30° to 150° on a MALLS instrument (BI-200SM/9000AT, Brookhaven Instruments Corporation). Astra software was used for data acquisition and analysis.

2.3. Surface modification of RO membranes

Surface modification of the RO membrane was conducted via dip coating followed by chemical cross-linking. For a typical operation, 100 mL of mixed solution of terpolymers P(MDBAC-*r*-Am-*r*-HEMA) (200–10,000 mg L^{-1}), cross-linking reagent GA (0.3 wt%) and H_2SO_4 (pH=3) was prepared. Then the wet LCLE membrane, which was maintained in DI water at 25 °C, was soaked into the polymer solution for 2 min and the excess casting solution was drained off by the membrane being vertically fixed in air for 2 min at room temperature. Finally, the resulting composite membrane was obtained by chemical cross-linking of P(MDBAC-*r*-Am-*r*-HEMA) and GA at 50 °C for 2 h. The coated membranes from different coating concentrations were designated as M_1 (200 mg L^{-1}), M_2 (500 mg L^{-1}), M_3 (1000 mg L^{-1}), M_4 (3000 mg L^{-1}) and M_5 (10,000 mg L^{-1}). The membranes were rinsed thoroughly with DI water and stored in DI water before measurements.

2.4. RO membrane surface characterization

The chemical composition of the membrane surface was investigated by ATR-FTIR (Bruker TENSOR37, USA). For ATR-FTIR analysis of membrane samples, Irtran crystal was used at 45° angle of incidence. The XPS data were obtained on an AXIS-Ultra instrument Kratos Analytical (SHIMADZU, Japan) using monochromatic Al Kα radiation (225 W, 15 mA, 15 kV) and low-energy electron flooding for charge compensation. Binding energies were calibrated using C 1s hydrocarbon peak at 284.8 eV. The data were converted into VAMAS file format and imported into Casa XPS software package for curve-fitting.

Membranes were washed in DI water for 24 h and dried in vacuum. The samples surface were sputter coated for 20 s using an Au target. Images were taken on a field emission scanning electron microscopy (FE-SEM) (S-4800, Hitachi, Japan). Membrane surface morphology was also measured by atomic force microscopy (CSPM5500, Being Nano-Instruments, China) imaging and analysis, equipped with standard silicon nitride cantilever.

The zeta potentials were obtained using the streaming potential method. The experimental set-up has been described in our previous work [21]. The streaming potential values were obtained using 0.1 mmol L^{-1} KCl as the feed solution. The temperature was thermostat at 25 °C and the pH was adjusted in the range of 3–10. The membrane samples were equilibrated for at least 24 h in 0.1 mmol L^{-1} KCl solution before test. The zeta potential was calculated from the streaming potential using the Fairbrother Mastin equation [22].

Dynamic water contact angle measurements were performed with the sessile drop method using a contact angle meter (Drop Shape Analysis 100, KRUSS BmbH Co., Germany). A syringe with a needle diameter of 0.525 mm was used to place a water droplet of 2 μL on the membrane. Tangent lines to both sides of the droplet static image were generated and averaged by the software Drop Shape Analysis.

2.5. RO membrane performance measurements

All the measurements of thin-film composite RO membranes performance were conducted at 1.5 MPa using a 2000 mg L^{-1} NaCl solution at 25 °C and pH of 7.0 using a cross-flow-type apparatus. The test cell has an effective membrane area of 18.75 cm^2. Fig. 1 shows the schematic diagram of the RO membrane cell-testing apparatus and a cross-section image of the membrane test cell. Both permeate and retentate were recycled back to the feed tank during the tests. The salt rejection and permeation flux were measured at least three times for every membrane sample. The results are average of three samples. Salt rejection (R) was calculated from the following equation:

$$R = \left(1 - \frac{C_p}{C_f}\right) \times 100\% \quad (1)$$

where C_p and C_f are the salt concentrations (mg L^{-1}) of the permeate and the feed, respectively, which were measured by a conductance meter (EL30, METTLER TOLEDO, Switzerland). The flux (F) was calculated from the following equation:

$$F = \frac{V}{St} \quad (2)$$

where V is the penetration liquid volume (L), S is the effective surface area of membrane (m^2) and t is the penetration time (h).

2.6. Membrane chlorination experiments

Chlorine resistances of the pristine and the coated membranes were evaluated via the cross-flow permeation tests with an aqueous solution of 500 mg L^{-1} NaOCl at the conditions of 1.5 MPa, 25.0 °C (the conductivity of the solution was adjusted to 4000 μs cm^{-1} with sodium chloride). Both permeate and retentate were recycled back to the feed tank during the tests (Fig. 1). All the results were average of three samples, with each sample tested at least three times. Herein the permeate water flux for each membrane was determined by direct measurement of the permeate flow in terms of liter per square meter per hour (L m^{-2} h^{-1}).

2.7. Evaluation of antifouling properties

The antifouling properties of the membrane were evaluated by the cross-flow filtration technique of BSA solution under 1.5 Mpa pressure at 25 °C. First, an aqueous 2000 mg L^{-1} NaCl solution was filtered through the membrane for 1 h before recording the initial water flux (J_0). In each filtration cycle, a 2000 mg L^{-1} of NaCl solution was first filtrated through the membrane for 6 h. Then a mixed solution of 2000 mg L^{-1} of NaCl and 100 mg L^{-1} of BSA was filtrated for 6 h. Next, the membranes were rinsed thoroughly with DI water for 2 h. The 6 h NaCl and 6 h NaCl+BSA filtration was defined as a filtration cycle. The relative flux recovery (J_r) was

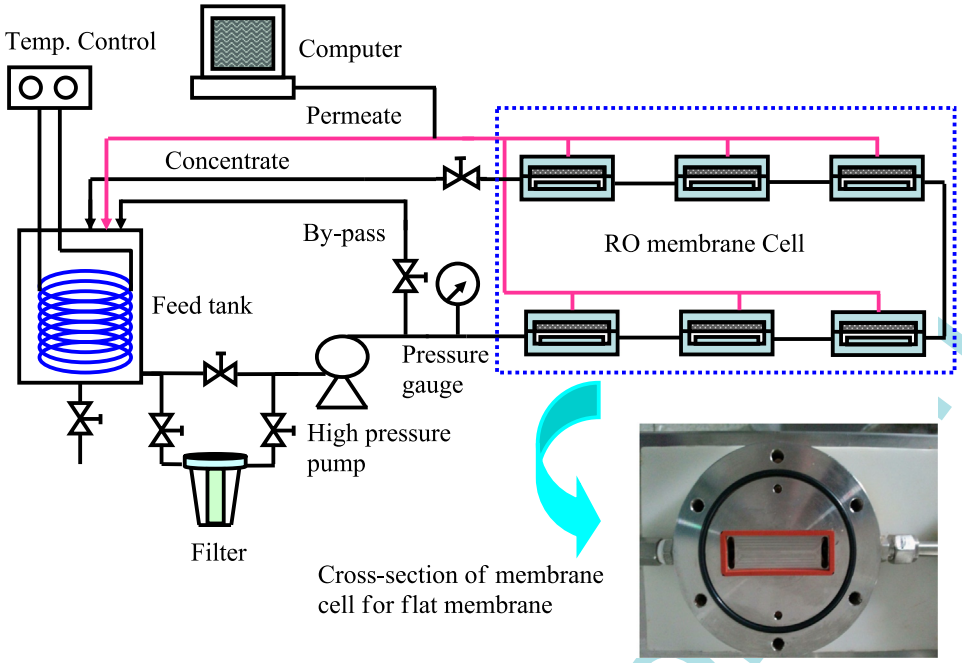

Fig. 1. Schematic diagram of RO membrane cell-testing apparatus and the cross-section of the membrane test cell.

obtained from the following equation:

$$J_r = J_t/J_0 \quad (3)$$

where J_0 and J_t are the initial flux and steady flux filtrating the BSA solution, respectively [6].

2.8. Evaluation of antimicrobial characteristics

Escherichia coli K12 was used as a model Gram-negative bacteria to evaluate antimicrobial properties of the membrane. Luria-Bertani (LB) broth is prepared by dissolving 1 wt% bacto-tryptone, 0.5 wt% yeast extract and 1 wt% NaCl in sterilized water. The aqueous solution's pH was adjusted to 7 by adding a 1 mol L^{-1} NaOH solution dropwise. LB agar plate is prepared by dissolving 1.5 wt% agar in LB broth. An overnight culture of *E. coli* was cultivated in LB broth in a shaking incubator (180 rpm) at 37 °C. 200 μL of the culture was then spread onto LB agar plates and LCLE or modified membrane (with a 2.54 cm diameter) followed by incubation for 24 h [10].

3. Results and discussion

Surface coating is easily implemented, so it is frequently used by the RO membrane industry for good antifouling performance and easy handling of the membrane. However, it used to lead to lowered membrane flux, despite the fact that flux loss can be minimized by optimizing the coating conditions [8,12,23,24]. As far as this phenomenon is concerned, we use a typical commercial low-energy RO membrane LCLE, which has a high permeation flux, as the starting membrane to compensate for the flux loss in the coating process. It is anticipated that the coating process can be varied to produce membrane with the flux falling at the range of typical standard brackish water RO (BWRO) membranes. In this study, a classic BWRO membrane BW30 was used as a control membrane for comparison.

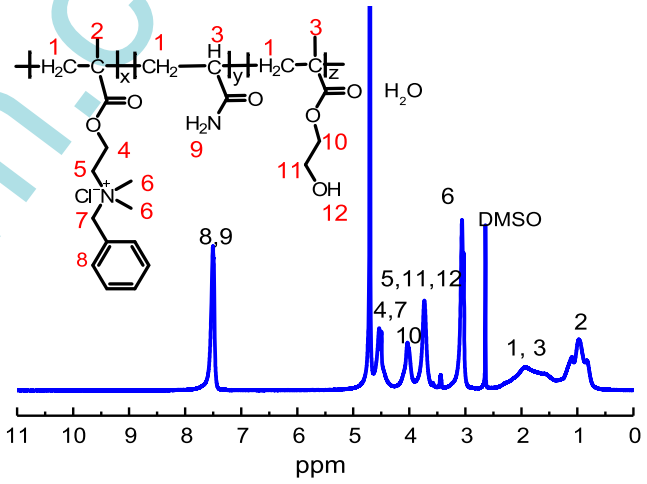

Fig. 2. ^{1}H NMR spectrum of P(MDBAC-*r*-Am-*r*-HEMA).

3.1. Synthesis of the coating material

The synthetic route for copolymer P(MDBAC-*r*-Am-*r*-HEMA) is outlined in Scheme 1. The chemical structure of the resultant copolymer was characterized by ^{1}H NMR and the ^{1}H NMR spectrum is shown in Fig. 2. The peaks in the 1.38–1.90 ppm and 1.78–2.45 ppm region are attributed to $-CH_2-$ and $-CH-$ in the polymer backbone, while the peaks at 0.70–1.25 ppm are assigned to methyl group in methacrylate units. The peak centered at 3.08 ppm corresponds to the protons of the $[(CH_3)_2N-]$ group in MDBAC units. The peaks 7.15–7.65 ppm are assigned to protons in the primary amide ($-CONH_2$) and benzene ring. The monomer ratio of MDBAC:Am:HEMA was calculated to be about 1:1:1 by comparing the intensity of these peaks. This ratio is similar to the feed ratio, indicating the similar free radical polymerization reactivity of these three monomers. Weight average molecular weight (M_w) of the terpolymer was calculated to be 67,000g mol L^{-1}, indicating high efficiency of the polymerization.

3.2. Effects of surface coating on RO membrane performance

To optimize the coating conditions, the P(MDBAC-*r*-Am-*r*-HEMA) solution concentration was used as the independent variable to investigate its effect on coated membrane performance. Fig. 3 shows the variation of permeation flux and salt rejection of membranes with the coating concentration. It is apparent that the coated membranes have decreased flux and improved salt rejection compared to the pristine LCLE membrane. The decreased flux is believed to be due to the increased membrane resistance caused by the coated polymer while the improved salt rejection is due to the sealing of the defective pores by the coated polymer which excludes the convective transport of salt ions [25]. It is interesting to see that the flux actually increases and then decreases while the salt rejection monotonically increases with the coating concentration. A similar phenomenon has been observed that higher permeation flux can be obtained at low coating concentrations of hydrophilic polymers. This may be due to the increased surface hydrophilicity at low coating concentrations where the filtration resistance has not been added. It should be mentioned that BW30 was used as a control membrane, showing typically performance of standard BWRO membranes. It can be seen that the coated membranes have similar flux but higher rejection than the BW30 membrane, indicating that it is feasible to prepare standard BWRO membranes with fair performance via the coating treatment of LERO membranes.

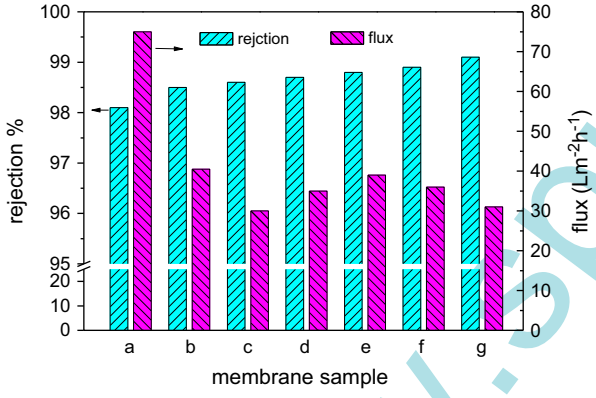

Fig. 3. Water flux and salt rejection for the virgin and modified membranes. Test conditions employed: 2000 mg L^{-1} NaCl aqueous solution, 1.5 MPa, 25.0 °C and pH 7.0 ((a)LCLE, (b) BW30, (c) M_1, (d) M_2, (e) M_3, (f) M_4 and (g) M_5).

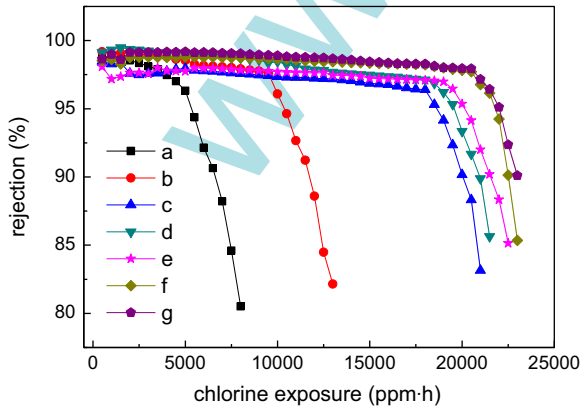

Fig. 4. Salt rejection for the virgin and modified PA membranes chlorinated under 500 ppm NaOCl at pH=11.0, 1.5 MPa, 25.0 °C. ((a) LCLE, (b) BW30, (c) M_1, (d) M_2, (e) M_3, (f) M_4 and (g) M_5).

3.3. Chlorine resistance of coated membranes

The chlorine resistance of virgin and modified membranes was evaluated by cross-flow filtration of NaOCl/NaCl solutions. The variations of salt rejection and permeation flux of membranes with chlorine exposure at pH of 11.0 are shown in Figs. 4 and 5. Both the virgin and modified membranes show excellent salt rejections, which are over 98.5%, during the first 6 h of operation. However, a

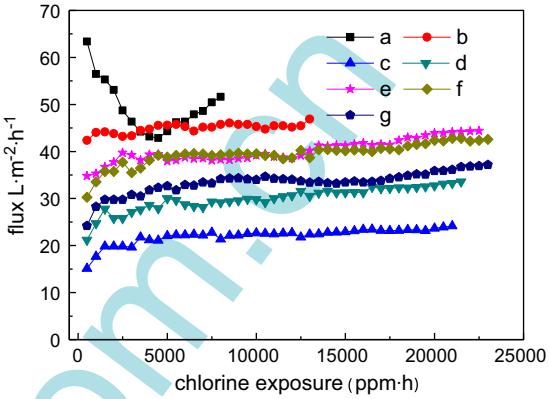

Fig. 5. Water flux for the virgin and modified PA membranes chlorinated under 500 ppm NaOCl at pH=11.0, 1.5 MPa, 25.0 °C. ((a) LCLE, (b) BW30, (c) M_1, (d) M_2, (e) M_3, (f) M_4 and (g) M_5).

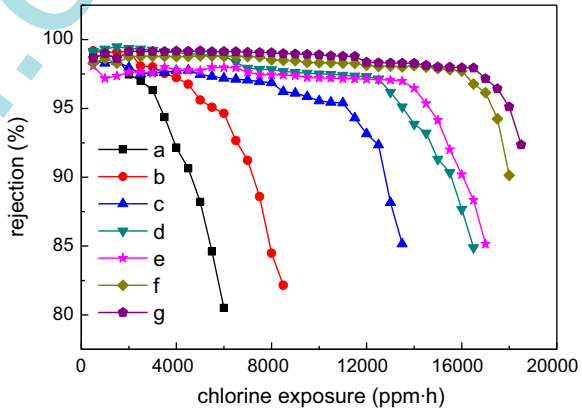

Fig. 6. Salt rejection for the virgin and modified PA membranes chlorinated under 500 mg L^{-1} NaOCl at pH=7.0, 1.5 MPa, 25.0 °C. ((a) LCLE, (b) BW30, (c) M_1, (d) M_2, (e) M_3, (f) M_4 and (g) M_5).

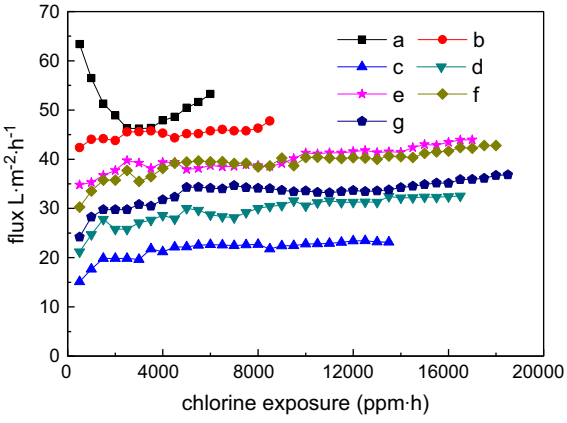

Fig. 7. Water flux for the virgin and modified PA membranes chlorinated under 500 mg L^{-1} NaOCl at pH=7.0, 1.5 MPa, 25.0 °C. ((a) LCLE, (b) BW30, (c) M_1, (d) M_2, (e) M_3, (f) M_4 and (g) M_5).

sharp decline of the salt rejection was observed at 6000 ppm h chlorine exposure for LCLE membrane and at 10,000 ppm h exposure for BW30 membrane. On the other hand, the modified membranes maintained its selectivity until the chlorine exposure level reached 23,000 ppm h, with the membrane prepared from the highest coating concentration (M_5) showing the best chlorine resistance.

Considering that the normal RO operating pH is 7–9, the chlorine exposure experiments were also conducted with the pH of NaClO solution adjusted to 7.0. The variation of membrane performance with the filtration time is shown in Figs. 6 and 7. It can be seen that both the rejection and flux plots show similar profiles as those at pH of 11. The membrane flux slowly increases while the rejection is stable initially and then drops off at some extent of chlorine exposure. It is noteworthy that although the rejection of membranes falls at the same sequence as that at pH of 11.0, all the membranes have the rejection decline coming earlier.

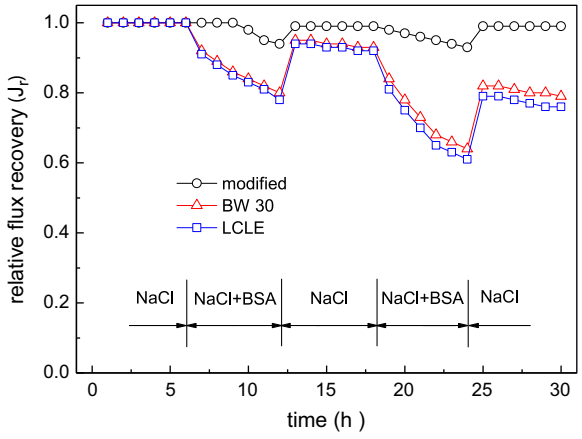

Fig. 8. Time-dependent relative flux recovery of unmodified and modified membranes for aqueous 2000 mg L^{-1} NaCl and 2000 mg L^{-1} NaCl+100 mg L^{-1} BSA solution with pH 4.7 ± 0.1((a) BW30, (b) LCLE and (c) M_3).

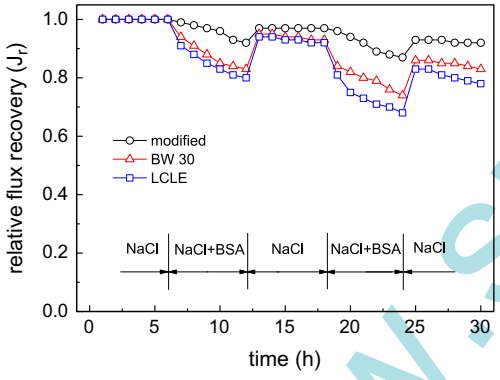

Fig. 9. Time-dependent relative flux recovery of unmodified and modified membranes for aqueous 2000 mg L^{-1} NaCl and 2000 mg L^{-1} NaCl+100 mg L^{-1} BSA solution with pH 7.0 ± 0.1((a) BW30, (b) LCLE and (c) M_3).

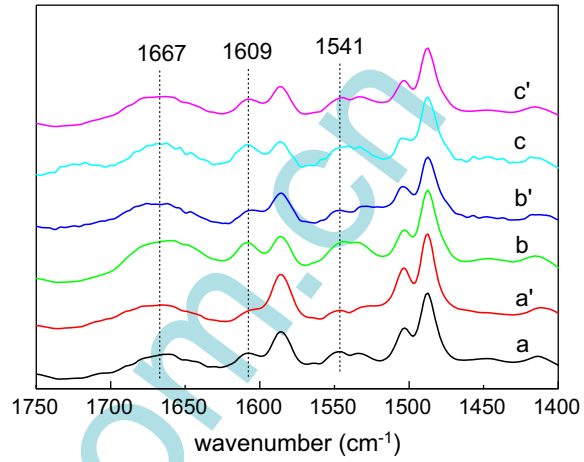

Fig. 11. ATR-FTIR spectra of the polyamide membrane: (a) BW30, (a′) BW30 pH=11/13,000 ppm h NaOCl, (b) LCLE, (b′) LCLE pH=11/13,000 ppm h NaOCl, (c) M_3, (c′) M_3 pH=11/13,000 ppm h NaOCl.

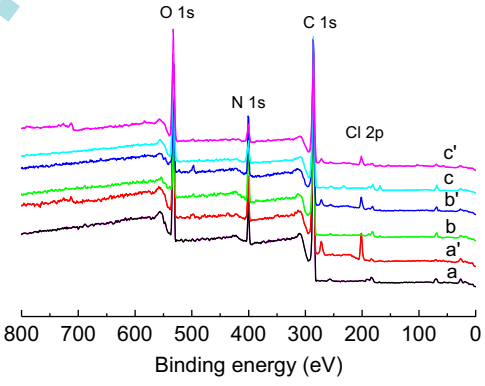

Fig. 12. The XPS survey scans of the polyamide membrane: (a) BW30, (b) BW30 pH=11+13,000 ppm h NaOCl, (c) LCLE, (d) LCLE *pH*=11/13,000 ppm h NaOCl, (e) M_3 and (f) M_3 pH=11/13,000 ppm h NaOCl.

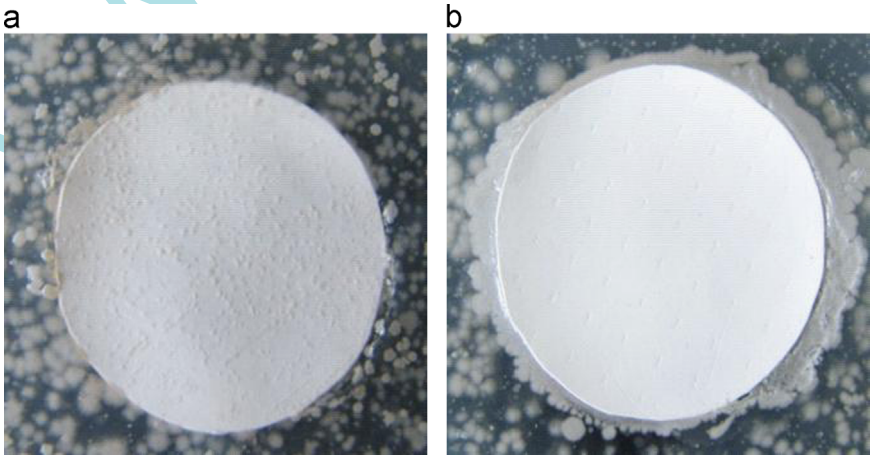

Fig. 10. Photographs showing *E. coli* growth on the surface of LCLE membrane (a) and M_3 membrane (b).

This corresponds with previous reports that chlorine can deteriorate RO membrane quicker at acid conditions. Despite this, the coated membranes still have much better resistance than LCLE and BW30 membranes. The tolerance limit of M_5 membrane is about 16,000 ppm h while those of LCLE and BW30 are 1500 ppm h and 3000 ppm h, respectively.

3.4. Antifouling performance of coated membranes

Non-specific adsorption is the start of almost all the fouling mechanisms; BSA, which is one of the stickiest proteins, was chosen as a model foulant. The antifouling properties of the membranes were evaluated by the cycled cross-flow filtration of BSA/NaCl solutions. Fig. 8 shows the variation of the relative flux as a function of filtration time. The pH value of the feed solution (2000 mg L^{-1} NaCl and 2000 mg L^{-1} NaCl + 100 mg L^{-1} BSA aqueous solution) was adjusted at 4.7 ± 0.1, which is the isoelectric point of BSA supposed to provoke the most severe hydrophobic–hydrophobic interaction. It can be seen that both BW30 and LCLE have much higher flux decline than the coated membranes when exposed to the BSA/NaCl solution. In addition, the coated membranes show higher flux recovery after membrane rinsing. The coated membranes maintain almost the same flux as the initial flux while LCLE and BW30 membranes lost 20% of the initial flux after filtration cycles, indicating irreversible fouling. Both the low flux decline under BSA filtration and the flux regeneration capacity of M_3 show better antifouling performance of coated membranes.

Table 1
Elemental compositions of virgin and modified membranes by XPS.

Membrane	[NaOCl] (mg L^{-1})	Soaking time (h)	Atomic concentration %			
			C 1s	N 1s	O 1s	Cl 2p
BW30	0	0	74.99	6.75	17.82	–
	500	24	71.18	7.14	19.38	1.63
LCLE	0	0	74.54	12.47	12.52	–
	500	24	71.48	11.97	13.57	2.93
Modified	0	0	72.83	6.47	19.27	–
	500	24	69.93	5.51	22.61	1.65

Considering the normal RO operating pH is 7–9, the BSA filtration experiments were also conducted at pH of 7.0 and the results are shown in Fig. 9. It can be seen that although both BW30 and LCLE membranes were fouled less, all the membranes show very similar flux profiles to those at pH of 4.7. It should be noted that even the coated membrane surface and BSA have appositive charges at pH 7.0; the antifouling performance of coated membranes is not discounted. The possible reason can be that the total exposure time to BSA in the fouling experiments is not enough for the electrostatic interaction, showing obvious effects on the flux profile, compared with other reports specifically investigating protein fouling mechanisms [26].

Since ammonium moiety has been copolymerized into the coating polymer, the antimicrobial activity of the membrane was evaluated separately. *E. coli* was chosen for the experiment because it is one of the most abundant bacteria in wastewater. Fig. 10 shows the cultured *E. coli* images on membrane surfaces. It can be seen that *E. coli* grew very well on the LCLE membrane so that the multiplied cells appeared as turbid white nodules in the

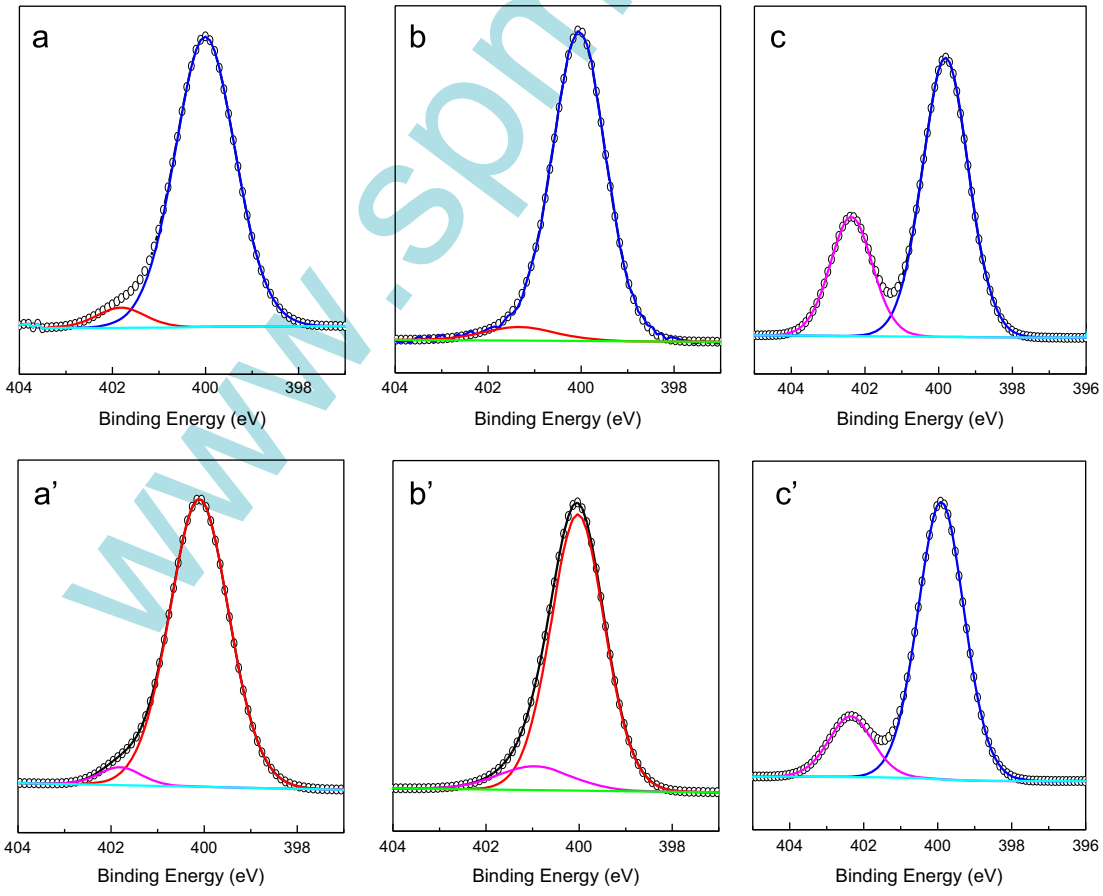

Fig. 13. High-resolution XPS spectra and deconvoluted peak assignments of N 1s for the polyamide membrane: (a) BW30, (a′) BW30 pH = 11/13,000 ppm h NaOCl, (b) LCLE, (b′) LCLE pH = 11/13,000 ppm h NaOCl, (c) M_3, (c′) M_3 pH = 11/13,000 ppm h NaOCl.

image (Fig. 10-a). However, very clean surface for the modified membrane (Fig. 10-b) was observed without any visible cell aggregates, indicating that the surface coating on the membrane effectively inhibited *E. coli* growth [10]. It should be mentioned that because the ammonium moiety only locates on the membrane surface rather than in the bulk material, bacteriostatic ring was not observed around the membrane.

3.5. Surface analysis

To better understand the effects of surface coating on membrane performance and the mechanism of the coating improving antifouling and chlorine-resistance of the RO membrane, the structure, morphology and physico-chemical properties of the membrane surface were analyzed in detail. As M_3 has the best rejection and permeation performances, it was chosen as a typical coating membrane for comparison.

3.5.1. Chemical structures

The chemical composition of the membrane surface was analyzed by ATR-FTIR. The ATR-FTIR spectra of virgin and chlorinated BW30, LCLE and M_3 are shown in Fig. 11. As for the spectra of BW30, LCLE and M_3, the absorption at 1541 cm^{-1} is mainly contributed by N–H bending motion (amide II) and the absorption at 1667 cm^{-1} is contributed by C═O stretch (amide I). The absorption at 1609 cm^{-1} is associated with the hydrogen-bonded carbonyl of the amide. These absorptions are characteristic of the PA layer of TFC membranes. As for the spectra of the chlorinated membranes, both BW30 and LCLE show great depression of the absorption at 1541 cm^{-1} and 1609 cm^{-1}, indicating replacement of hydrogen of the amide nitrogen with chlorine due to the electrophilic substitution in N-chlorination. By contrast, the change on these absorptions for M_3 due to chlorination is minimal, which suggests the robustness of the amide structure to chlorine exposure in the M_3 membrane.

The chemical composition of the virgin and chlorinated membranes was also analyzed by XPS. The XPS wide scans of the membrane surfaces are shown in Fig. 12. All the spectra of virgin membranes have peaks at 530 eV, 400 eV and 285 eV, which can be assigned to oxygen, nitrogen and carbon, respectively. For the spectra of chlorinated membranes, the new peaks at 200 eV and 270 eV are due to the chlorine atom attached to the polyamide membrane. This indicates that all of the membranes have chemically bonded chlorine and none of them is absolved of chlorine stack. Table 1 shows the element contents of the membrane surface. It can be seen that the LCLE membrane has a nitrogen content of 12.4%, which is within those of total linear (9.5%) and totally cross-linked (12.5%) polyamide material, indicating a "naked" PA surface. The BW30 membrane has a

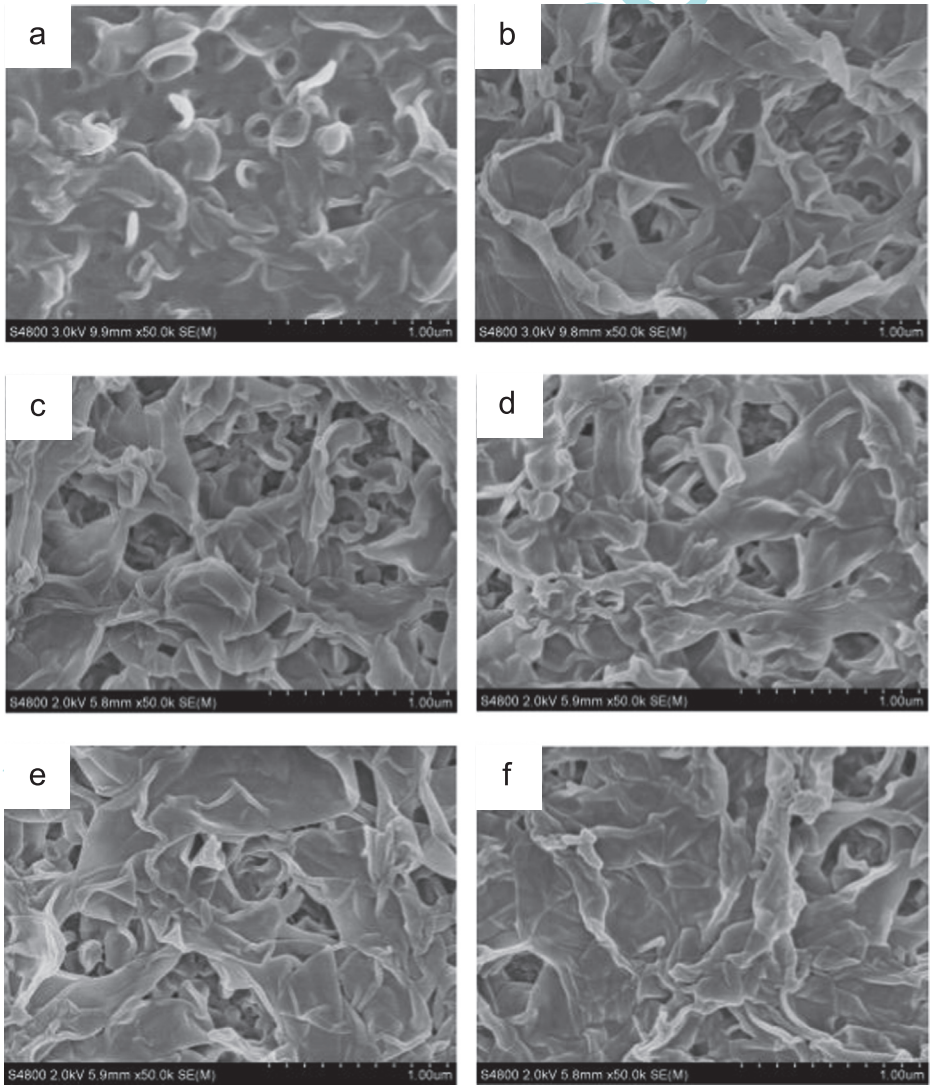

Fig. 14. SEM images of the surface of unmodified TFC membrane ((a) BW30 and (b) LCLE) and modified membranes ((c) M_1, (d) M_2, (e) M_3, (f) M_4).

much higher oxygen content (17.82%). This is believed to be due to the presence of a coating layer rich in oxygen, which is reported to be poly(vinyl alcohol) (PVA) by other literature [27]. The membrane M_3 has the highest oxygen content (19.27%), which is aroused by the coated polymer. It can also be seen that all the chlorinated membranes have the signal attributed to Cl 2p, with LCLE having the highest content. This indicates the LCLE membrane was most severely attacked by chlorine. The chlorinated BW30 and M_3 have similar chlorine contents. However, it can be seen from the chlorine exposure results of BW30 that the PVA coating could not protect the PA film under the chlorination conditions applied in this study. On the other hand, for the M_3 membrane, it is believed that the coated polymer can preferentially react with chlorine rather than just working as a physical barrier, precluding the contact of chlorine with the PA film.

The high-resolution XPS spectra for N of virgin and chlorinated (500 mg $L^{-1} \times 24$ h, pH = 11.0) membranes are illustrated in Fig. 13. Changes in chemical bonding at the surface of the PA layer can be understood through analysis of the shifts in the binding energy (BE) of the deconvoluted peak spectra. The N 1s peak can be curve-fitted with two peak components at BEs of 399.6 and 402.5 eV (Fig. 13-c), attributed to C–N and –N $(R)_4^+$, respectively [28,29]. For the BW30 and LCLE membrane, the presence of the deconvoluted N 1s peak at 402.5 eV is due to the protonation of the residue amine in the PA film. For the coated membrane M_3, the signal of this peak significantly increases, indicating the successful coating of P(MDBAC-*r*-Am-*r*-HEMA).

3.5.2. Surface morphologies

The morphology of membrane surfaces was analyzed by SEM and AFM. The SEM results are shown in Fig. 14. It can be seen that the virgin thin-film composite polyamide membrane has a typical ridge-and-valley structure. No dramatic change on the surface morphology was observed from the surface coating. Only when P(MDBAC-*r*-Am-*r*-HEMA) was used at its highest content, the "valley" structures appear filled by the coated polymer and the membrane surface becomes smoother. The AFM results are shown in Fig. 15. It can also be seen that the nodules on the membrane surface become bigger with the increase in coating concentration and then melted with each other. The surface roughness data shown in Table 2 also indicate that the root-mean-square (R_{rms}) and peak-to-valley distance (R_{p-v}) values of the membrane surface first increase and then decrease with the coating concentration.

3.5.3. Hydrophilicity

It is known that the membrane surface hydrophilicity is one of the most important factors influencing membrane performance. In our study, the dynamic water contact angle (WCA) was measured for unmodified and modified membranes. As shown in Fig. 16, the modified membranes show much better wettabilities than the

Table 2
Surface roughness of the virgin and modified membranes.

Membrane samples	R_a(nm)	R_{rms} (nm)	R_{p-v} (nm)
BW30	33.6	42.8	350
LCLE	47.2	60.1	465
M_2	54.1	67.6	484
M_3	64.9	81.8	584
M_4	53.1	66.7	548
M_5	50.7	64.5	490

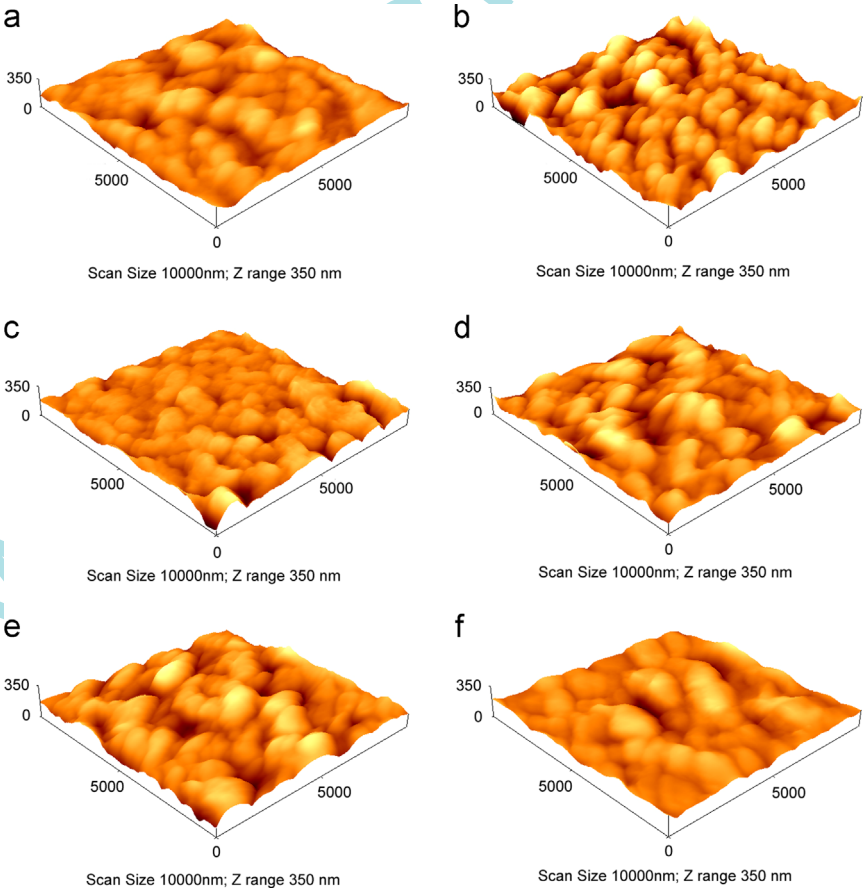

Fig. 15. AFM images of unmodified membrane ((a) BW30 and (b) LCLE) and modified membranes ((c) M_2, (d) M_3, (e) M_4 and (f) M_5). The size of the images is 10 μm × 10 μm. The *Z* (gray) scale is 350 nm.

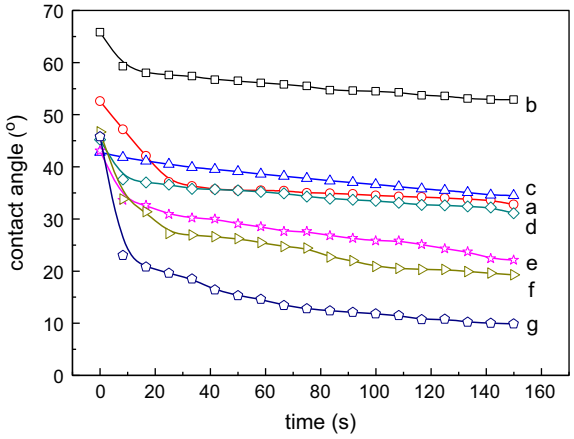

Fig. 16. Dynamic water contact angle measurements for unmodified membrane ((a) BW30 and (b) LCLE) and modified membranes ((c) M_1, (d) M_2, (e) M_3, (f) M_4 and (g) M_5).

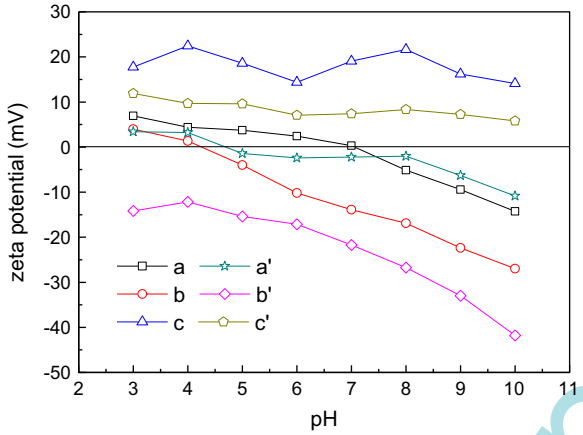

Fig. 17. Zeta potential for virgin and chlorinated ((a) BW30, (b) LCLE, (c) M_3, (d) BW30/pH=11 NaOCl 13,000 ppm h, (e) LCLE pH=11/13,000 ppm h, (f) M_3 pH=11/13,000 ppm h NaOCl).

unmodified ones. The WCA values of BW30 and LCLE at 30 s were 35.3° and 57° respectively, whereas the value of M_5 decreased to 18°. In addition, the WCA of modified membranes decreases with the coated P(MDBAC-*r*-Am-*r*-HEMA) content. The improvement of membrane surface hydrophilicity is believed to benefit the anti-fouling performance of membranes.

3.5.4. *Surface charge*

Surface charge properties of BW30, LCLE and modified membranes before and after chlorination are measured by the streaming method [30]. The results are presented in Fig. 17. It can be seen that both BW30 and LCLE show the typical amphoteric characteristic for TFC RO membranes, with the positive charge contributed by the residue amine group and the negative charge contributed by the residue carboxylic group. It can also be seen that BW30 has a quite neutral surface and LCLE is slightly negatively charged at neutral pH. The modified membrane has a positively charged surface at the whole pH range, indicating successful immobilization of the hydrophilic polymer on the membrane surface and the presence of a large amount of ammonium cations. Similar to our observation in a previous study, all the chlorinated membranes have more negative surfaces than the virgin membranes [21]. One reason can be the consumption of amine groups, which are resources of the positive charge. The other reason can be the partial hydrolysis of the amide group promoted by the chlorination reaction [27].

4. Conclusions

In this work, a surface coating method was developed to prepare RO membranes with improved chlorine and fouling resistance. The method is simple as it is based on dip coating and cross-linking of a hydrophilic polymeric material on a commercial TFC RO membrane. The coating material is prepared by traditional free radical polymerization in solution, which enables convenient choosing of the chemical moieties with the required moieties, such as antimicrobial properties and preferential reactivity with chlorines, onto the membrane surface. The method is efficient as the resulted membranes show much better wettability, antimicrobial properties, chlorine and fouling resistances than the virgin membranes, with the membranes prepared from higher coating concentration showing more prominent effects. The surface analysis indicates that the surface coating has significantly varied the physicochemical properties of the membrane surface. A trade-off has been observed between the membrane flux and the coating effects improving chlorine and fouling resistances of membranes. Therefore, the coating concentration was used as an independent variable to optimize the resulting membrane performance. It should be noted that the microstructure and chemical composition of the coated polymer could be optimized to further improve the resulting membrane performance. This work is under way in our lab and will be reported in due course.

Acknowledgments

The authors gratefully acknowledge the financial support by The National Nature Science Foundation of China (Grant no. 21274108) and the National High Technology Research and Development Program of China (863 Program of China, 2012AA03A602). Prof. MJQ also thanks Prof. Benny Freeman (University of Texas at Austin, USA) and Dr. Geoffrey Geise (Penn State University, USA) for helpful discussions.

References

[1] I.D. Association, Desalination Yearbook 2011-2012, 2012.
[2] J.E. Cadotte, R.J. Petersen, R.E. Larson, E.E. Erickson, A new thin-film composite seawater reverse osmosis membrane, Desalination 32 (1980) 25–31.
[3] N. Misdan, W.J. Lau, A.F. Ismail, Seawater Reverse Osmosis (SWRO) desalination by thin-film composite membrane – current development, challenges and future prospects, Desalination 287 (2012) 228–237.
[4] G.D. Kang, Y.M. Cao, Development of antifouling reverse osmosis membranes for water treatment: a review, Water Research 46 (2012) 584–600.
[5] Y.J. Kim, K.S. Lee, M.H. Jeong, J.S. Lee, Highly chlorine-resistant end-group crosslinked sulfonated-fluorinated poly(arylene ether) for reverse osmosis membrane, Journal of Membrane Science 378 (2011) 512–519.
[6] Y.L. Ji, Q.F. An, Q. Zhao, W.D. Sun, K.R. Lee, H.L. Chen, C.J. Gao, Novel composite nanofiltration membranes containing zwitterions with high permeate flux and improved anti-fouling performance, Journal of Membrane Science 390 (2012) 243–253.
[7] L. Zou, I. Vidalis, D. Steele, A. Michelmore, S.P. Low, J.Q.J.C. Verberk, Surface hydrophilic modification of RO membranes by plasma polymerization for low organic fouling, Journal of Membrane Science 369 (2011) 420–428.
[8] R.A. Al-Juboori, T. Yusaf, Biofouling in RO system: mechanisms, monitoring and controlling, Desalination 302 (2012) 1–23.
[9] Y.F. Yang, H.-Q. Hu, Y. Li, L.-S. Wan, Z.-K. Xu, Membrane surface with antibacterial property by grafting polycation, Journal of Membrane Science 376 (2011) 132–141.
[10] Y.H. La, B.D. McCloskey, R. Sooriyakumaran, A. Vora, B. Freeman, M. Nassar, J. Hedrick, A. Nelson, R. Allen, Bifunctional hydrogel coatings for water purification membranes: Improved fouling resistance and antimicrobial activity, Journal of Membrane Science 372 (2011) 285–291.
[11] J. Glater, S. kwan Hong, M. Elimelech, The search for a chlorine-resistant reverse osmosis membrane, Desalination 95 (1994) 325–345.

[12] Y.-N. Kwon, J.O. Leckie, Hypochlorite degradation of crosslinked polyamide membranes: I. Changes in chemical/morphological properties, Journal of Membrane Science 283 (2006) 21–26.
[13] Y.-N. Kwon, J.O. Leckie, Hypochlorite degradation of crosslinked polyamide membranes: II. Changes in hydrogen bonding behavior and performance, Journal of Membrane Science 282 (2006) 456–464.
[14] C.H. Lee, J. Spano, J.E. McGrath, J. Cook, B.D. Freeman, S. Wi, Solid-State NMR molecular dynamics characterization of a highly chlorine-resistant disulfonated poly(arylene ether sulfone) random copolymer blended with poly (ethylene glycol) oligomers for reverse osmosis applications, Journal of Physical Chemistry B 115 (2011) 6876–6884.
[15] T. Shintani, H. Matsuyama, N. Kurata, Development of a chlorine-resistant polyamide reverse osmosis membrane, Desalination 207 (2007) 340–348.
[16] G.D. Kang, C.J. Gao, W.D. Chen, X.M. Jie, Y.M. Cao, Q. Yuan, Study on hypochlorite degradation of aromatic polyamide reverse osmosis membrane, Journal of Membrane Science 300 (2007) 165–171.
[17] R.H. Du, J.S. Zhao, Properties of poly (N,N-dimethylaminoethyl methacrylate)/polysulfone positively charged composite nanofiltration membrane, Journal of Membrane Science 239 (2004) 183–188.
[18] D.H. Shin, N. Kim, Y.T. Lee, Modification to the polyamide TFC RO membranes for improvement of chlorine-resistance, Journal of Membrane Science 376 (2011) 302–311.
[19] M.H. Liu, Z.W. Chen, S.C. Yu, D.H. Wu, C.J. Gao, Thin-film composite polyamide reverse osmosis membranes with improved acid stability and chlorine resistance by coating N-isopropylacrylamide-co-acrylamide copolymers, Desalination 270 (2011) 248–257.
[20] X. Wei, Z. Wang, J. Chen, J. Wang, S. Wang, A novel method of surface modification on thin-film-composite reverse osmosis membrane by grafting hydantoin derivative, Journal of Membrane Science 346 (2010) 152–162.
[21] X.F. Zhai, J.Q. Meng, R. Li, L. Ni, Y.F. Zhang, Hypochlorite treatment on thin film composite RO membrane to improve boron removal performance, Desalination 274 (2011) 136–143.
[22] M. Elimelech, W.H. Chen, J.J. Waypa, Measuring the zeta (electrokinetic) potential of reverse osmosis membranes by a streaming potential analyzer, Desalination 95 (1994) 269–286.
[23] S.C. Yu, X.S. Liu, J.Q. Liu, D.H. Wu, M.H. Liu, C.J. Gao, Surface modification of thin-film composite polyamide reverse osmosis membranes with thermo-responsive polymer (TRP) for improved fouling resistance and cleaning efficiency, Separation and Purification Technology 76 (2011) 283–291.
[24] D.H. Wu, X.S. Liu, S.C. Yu, M.H. Liu, C.J. Gao, Modification of aromatic polyamide thin-film composite reverse osmosis membranes by surface coating of thermo-responsive copolymers P(NIPAM-co-Am). I: Preparation and characterization, Journal of Membrane Science 352 (2010) 76–85.
[25] C.Y. Tang, Y.N. Kwon, J.O. Leckie, Effect of membrane chemistry and coating layer on physiochemical properties of thin film composite polyamide RO and NF membranes II. Membrane physiochemical properties and their dependence on polyamide and coating layers, Desalination 242 (2009) 168–182.
[26] Y. Wang, C.Y. Tang, Protein fouling of nanofiltration, reverse osmosis, and ultrafiltration membranes – the role of hydrodynamic conditions, solution chemistry, and membrane properties, Journal of Membrane Science 376 (2011) 275–282.
[27] V.T. Do, C.Y.Y. Tang, M. Reinhard, J.O. Leckie, Degradation of polyamide nanofiltration and reverse osmosis membranes by hypochlorite, Environmental Science and Technology 46 (2012) 852–859.
[28] Y. Wang, J.Y. Qiu, J. Peng, L. Xu, J.Q. Li, M.L. Zhai, Study on the chemical stability of the anion exchange membrane of grafting dimethylaminoethyl methacrylate, Journal of Membrane Science 376 (2011) 70–77.
[29] J.Y. Qiu, M.L. Zhai, J.H. Chen, Y. Wang, J. Peng, L. Xu, J.Q. Li, G.S. Wei, Performance of vanadium redox flow battery with a novel amphoteric ion exchange membrane synthesized by two-step grafting method, Journal of Membrane Science 342 (2009) 215–220.
[30] F. Yao, G.-D. Fu, J. Zhao, E.-T. Kang, K.G. Neoh, Antibacterial effect of surface-functionalized polypropylene hollow fiber membrane from surface-initiated atom transfer radical polymerization, Journal of Membrane Science 319 (2008) 149–157.